Journal of Radiation Research, Vol. 62, No. 5, 2021, pp. 926–933
https://doi.org/10.1093/jrr/rrab054
Advance Access Publication: 1 July 2021

Prediction of target position from multiple fiducial markers by partial least squares regression in real-time tumor-tracking radiation therapy

Kanako Ukon[1], Yohei Arai[2], Seishin Takao[3,4], Taeko Matsuura[3,4], Masayori Ishikawa[5], Hiroki Shirato[6], Shinichi Shimizu[3,6], Kikuo Umegaki[4] and Naoki Miyamoto[3,4,*]

[1]Graduate School of Medicine, Hokkaido University, North 15, West 7, Kita-ku, Sapporo, Hokkaido 060-8638, Japan
[2]Graduate School of Engineering, Hokkaido University, North 13, West 8, Kita-ku, Sapporo, Hokkaido 060-8628, Japan
[3]Department of Medical Physics, Hokkaido University Hospital, North 14, West 5, Kita-ku, Sapporo, Hokkaido 060-8648, Japan
[4]Faculty of Engineering, Hokkaido University, North13, West 8, Kita-ku, Sapporo, Hokkaido 060-8628, Japan
[5]Faculty of Health Sciences, Hokkaido University, North12, West 5, Kita-ku, Sapporo, Hokkaido 060-0812, Japan
[6]Faculty of Medicine, Hokkaido University, North 15, West 7, Kita-ku, Sapporo, Hokkaido 060-8638, Japan
*Corresponding author: Faculty of Engineering, Hokkaido University, North 13, West 8, Kita-ku, Sapporo, Hokkaido 060-8638, Japan. Tel: +81-11-706-6673, E-mail address: miya-nao@eng.hokudai.ac.jp
(Received 19 January 2021; revised 24 March 2021; editorial decision 21 June 2021)

ABSTRACT

The purpose of this work is to show the usefulness of a prediction method of tumor location based on partial least squares regression (PLSR) using multiple fiducial markers. The trajectory data of respiratory motion of four internal fiducial markers inserted in lungs were used for the analysis. The position of one of the four markers was assumed to be the tumor position and was predicted by other three fiducial markers. Regression coefficients for prediction of the position of the tumor-assumed marker from the fiducial markers' positions is derived by PLSR. The tracking error and the gating error were evaluated assuming two possible variations. First, the variation of the position definition of the tumor and the markers on treatment planning computed tomograhy (CT) images. Second, the intra-fractional anatomical variation which leads the distance change between the tumor and markers during the course of treatment. For comparison, rigid predictions and ordinally multiple linear regression (MLR) predictions were also evaluated. The tracking and gating errors of PLSR prediction were smaller than those of other prediction methods. Ninety-fifth percentile of tracking/gating error in all trials were 3.7/4.1 mm, respectively in PLSR prediction for superior–inferior direction. The results suggested that PLSR prediction was robust to variations, and clinically applicable accuracy could be achievable for targeting tumors.

Keywords: real-time tumor-tracking radiation therapy; fiducial marker; partial least squares regression (PLSR); tracking irradiation; gating irradiation

INTRODUCTION

Respiratory-induced tumor motion is one of the significant sources of uncertainty for lung, liver and other organs in the thoracic/abdominal region in radiation therapy. In order to treat mobile tumors by monitoring tumor position during treatment, real-time tumor-tracking radiation therapy (RTRT) [1–3] using internal fiducial markers and a gating irradiation technique have been clinically applied. Tracking irradiation techniques that change the irradiation position/field according to the tumor position by using electromagnetic transponder guided multileaf collimator (MLC) [4, 5], a compact linear accelerator mounted on a robotic arm [6, 7] and the gimbaled X-ray head [8, 9] have also been realized. These techniques utilize the internal fiducial markers and rely on the correlation between marker motion and tumor motion. Since the correlation between internal motion and external abdominal motion is not necessarily maintained [10, 11], it is effective to utilize the internal fiducial markers for monitoring the tumor motion directly. One of the methods to estimate the tumor position from the information of markers' positions is to create a prediction model which

derives a representative 3D position of the tumor from the markers' positions [12]. In order to build the prediction model, the use of four-dimensional computed tomography (4DCT) images acquired for treatment planning is one of the approaches used [13] since it is difficult to assess the 3D motion of a tumor and the surrounding markers with 2D images. The correlation of internal motion is complicated, however, it is possible that the prediction accuracy could be improved by using the multiple fiducial markers. One of the prediction models is multiple linear regression (MLR). However, in ordinary MLR prediction, since the correlation of internal motion is complicated, the predicted tumor position may fluctuate significantly by small input variation due to multicollinearity. There are few studies about the real-time target position prediction method using multiple fiducial markers.

In this study, we propose a prediction method based on a partial least squares regression (PLSR [14]) for monitoring the location of mobile tumors. In PLSR, explanatory variables are transformed into the variables that are uncorrelated with each other (called latent variables [LVs]) and regression coefficients are derived, hence multicollinearity problems can be avoided. By using some principle LVs, components that do not contribute to the prediction, such as noise, can be excluded from the regression model. In this study, the 3D coordinates of the three markers—nine parameters in total—are used for the prediction of tumor position. The purpose of this study is to show the usefulness of the proposed method in terms of tracking and gating errors with assuming the possible variations occurring in a clinical workflow. The trajectory data of fiducial markers obtained in lung RTRT was used for evaluation. The tracking and gating errors are compared with those estimated with rigid prediction and ordinary MLR prediction.

MATERIALS AND METHODS

Target position prediction by PLSR with multiple fiducial markers

In this study, it is assumed that the 3D coordinates of the tumor are predicted from the 3D coordinates of three markers, that is, by nine explanatory variables. First, the tumor coordinates $\boldsymbol{Y}(P)$ and the three fiducial markers coordinates $\boldsymbol{X}(P)$ in the treatment room coordinate system (x, y, z) with reference to isocenter are determined for each computed tomography (CT) data set of 4DCT as following:

$$\boldsymbol{Y}(P) = \left[Y_x(P), Y_y(P), Y_z(P) \right], \tag{1}$$

$$\begin{aligned} \boldsymbol{X}(P) = [&X_{1x}(P), X_{1y}(P), X_{1z}(P), X_{2x}(P), X_{2y}(P), \\ &X_{2z}(P), X_{3x}(P), X_{3y}(P), X_{3z}(P) \,], \end{aligned} \tag{2}$$

where P represents the respiratory phase in each CT data set. $\boldsymbol{Y}(P)$ is a column vector containing 3D coordinates of the tumor, and $\boldsymbol{X}(P)$ is a column vector containing nine marker coordinate data. The subscript numbers in equation (2) represent the identification number of the marker. When 4DCT data includes 10 respiratory phases, 10 pairs of $\boldsymbol{Y}(P)$ and $\boldsymbol{X}(P)$ are obtained. Next, constant 3D coordinate $\boldsymbol{C}$ is defined as the average position of the center of gravity of the three fiducial markers. By assuming 10 phases, $\boldsymbol{C}$ is represented by:

$$\boldsymbol{C} = \left[C_x, C_y, C_z \right], \tag{3}$$

$$C_x = \sum_{P=1}^{10} \left(\frac{X_{1x}(P) + X_{2x}(P) + X_{3x}(P)}{3} \right) / 10. \tag{4}$$

C_y and C_z are evaluated with same as C_x. Then, all coordinates are corrected with reference to $\boldsymbol{C}$ as:

$$\boldsymbol{Y}_c(P) = \boldsymbol{Y}(P) - \boldsymbol{C}, \tag{5}$$

$$\boldsymbol{X}_c(P) = \boldsymbol{X}(P) - [\boldsymbol{C}, \boldsymbol{C}, \boldsymbol{C}]. \tag{6}$$

$\boldsymbol{C}$ and $\boldsymbol{C}(t)$ shown after are necessary to correct the geometrical shift of the average position of the marker in the treatment room coordinate system due to the baseline-shift [15] of the tumor motion. Our objective is to find a linear model $\boldsymbol{Y}_c = \boldsymbol{X}_c\boldsymbol{B}$ where $\boldsymbol{B}$ is a matrix whose columns and rows are three and nine, respectively, including the nine regression coefficients for each axis. In this study, all analyses were performed using MATLAB (MathWorks Inc., USA), and $\boldsymbol{B}$ was derived by statistically inspired modification of the partial least squares (SIMPLS) algorithm. SIMPLS is one of the fast algorithms to derive the regression coefficients. The algorithm of SIMPLS is based on the singular value decomposition (SVD) of the cross product of inverse matrix of explanatory variables and matrix of response variables as represented by $\boldsymbol{X}_c^{-1}\boldsymbol{Y}_c$. LV is derived as a combination of the original explanatory variables during SVD process. The number of the LVs corresponds to the number of SVD process. Please refer to the literature [16] for details of the SIMPLS algorithm.

The 3D coordinate of the tumor during treatment, $\hat{\boldsymbol{Y}}(t)$, as a function of time t is predicted as follows:

$$\hat{\boldsymbol{Y}}(t) = \boldsymbol{X}_c(t)\boldsymbol{B} + \boldsymbol{C}(t), \tag{7}$$

where $\boldsymbol{X}_c(t)$ is the 3D coordinates expressed as:

$$\boldsymbol{X}_c(t) = \boldsymbol{X}(t) - \boldsymbol{C}(t), \tag{8}$$

where $\boldsymbol{X}(t)$ is the 3D coordinates of the three markers obtained during the treatment and $\boldsymbol{C}(t)$ is the average position of the center of gravity of the three fiducial markers during one respiratory cycle. In this way, the tumor position $\hat{\boldsymbol{Y}}(t)$ is predicted in real-time from the coordinates data of multiple markers.

In PLSR, the number of LVs should be determined in advance of prediction. The residual error in the training process could be reduced by increasing the number of LVs, however, the estimated value may fluctuate significantly in the validation process due to overfitting and multicollinearity. In order to use the optimal number of LVs according to each patient-specific condition, the mean prediction error (MPE) for each number of LVs is evaluated by leave-one-out cross-validation in the training process. In order to avoid overfitting and multicollinearity, the maximum number of LVs to derive the regression coefficients was set to 3, and the number of LVs that minimizes MPE was defined as the optimal number of LVs.

In a real-life situation, the tumor and the marker position defined in the CT images could include the variation due to the influence of motion artifacts and/or inter-operator variance. In addition, the geometrical relationship between the markers and the tumor in the body may be varied at the time of treatment from the acquisition of treatment planning CT due to intra-fractional anatomical variation

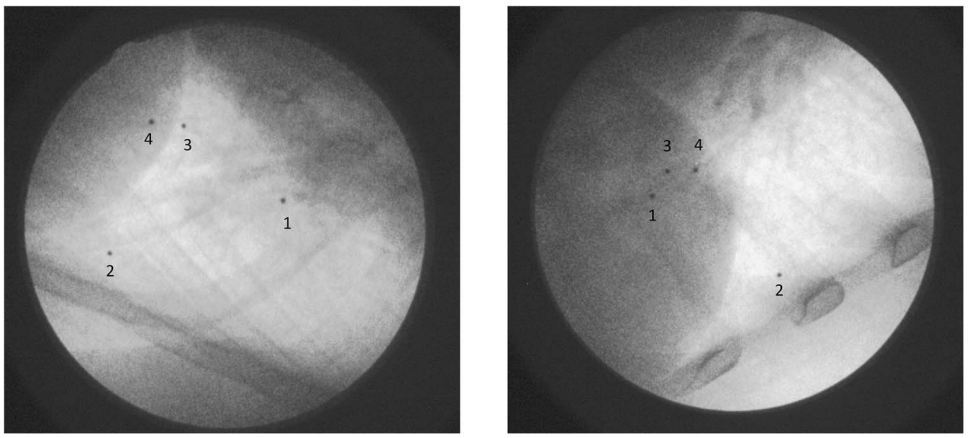

Fig. 1. An example of two fluoroscopic images obtained in lung RTRT. The fluoroscopic images were acquired from oblique direction to patient. Four internal fiducial markers are shown and identified by corresponding numbers. These images were taken from patient #9 showing the relatively large tracking error compared with other patients. The marker used in clinic was a sphere-shaped gold marker the diameter of which was 1.5 mm. The distance between marker 1 and marker 2 was 64.0 mm, between 1 and 3 it was 43.4 mm, between 1 and 4 it was 56.3 mm, between 2 and 3 it was 43.3 mm, between 2 and 4 it was 37.9 mm, and between 3 and 4 it was 15.0 mm.

and/or marker migration [17]. In this study, the tracking and gating errors are evaluated by assuming these variations in order to show the clinical feasibility and the effectiveness of the PLSR prediction. In the following, the clinical data and the procedure for the evaluation of the tracking and gating errors are described.

Patient data for evaluation

In this study, the trajectory data of respiratory motion of four internal fiducial markers inserted in lungs were used for the analysis. The data were obtained from 10 patients who underwent lung RTRT with SyncTraX (Shimadzu, Japan) [18] based on orthogonal stereoscopic X-ray imaging. The examples of two fluoroscopic images in lung RTRT are shown in Fig. 1. Three-dimensional positions of the markers were recorded at 30 times/sec. The trajectory data included at least one marker of which 3D motion range of more than 5 mm was selected. Table 1 shows summary of the trajectory data used for evaluation. The position of one of the four markers was assumed to be the tumor position and was predicted by the other three fiducial markers. By replacing the tumor assumed marker, one trajectory data simulated four situations in each prediction method. The trajectory data excluding the training data was used for the evaluation of prediction accuracy. The distance between the tumor assumed marker and the center of gravity of the three markers was 28.3 ± 10.5 mm. The distance was limited to 50 mm in order to avoid an extreme case which could not be applied in actual clinical situation. Since the distance between the gross tumor volume (GTV) center and the marker closest to the GTV was 25.3 ± 16.7 mm in the actual treatment, the distance between the tumor and the marker in the evaluation was thought to be equivalent to the clinical situation.

Evaluation of tracking error and gating error

Fig. 2 shows the overview including the training process and evaluation process of the tracking and gating errors. In the training process, in order to mimic the use of 4DCT, the data of the length of one respiratory cycle in the first part of the original log data obtained with 30 point/sec was resampled into 10 points/cycle which corresponded to the typical temporal resolution of 4DCT. The remaining log data was used for the evaluation.

In this study, the following two kinds of variations were reproduced. One is the variation of the position definition of the tumor and the markers on each CT data in 4DCT in the training process, represented by $\Delta \boldsymbol{Y}_{CT}(P)$ and $\Delta \boldsymbol{X}_{CT}(P)$. The other is the intra-fractional anatomical variation which induces the distance change between the tumor and markers from the treatment planning CT acquisition in the evaluation process, represented by $\Delta \boldsymbol{Y}_{intra}$ and $\Delta \boldsymbol{X}_{intra}$. In this study, the tracking error and the gating error were evaluated by means of a random sampling method which assumed that the probability of the above variations follow the normal distribution with a mean of 0. $\Delta \boldsymbol{Y}_{CT}(P)$ and $\Delta \boldsymbol{X}_{CT}(P)$ are given randomly for each respiratory phase according to the normal distribution $N\left(0, \sigma_{CT}^2\right)$. Here, σ_{CT} was defined as the 1/10 of motion range of training data, assuming that the motion artifact was the main factor of the variation in the determination of the tumor and markers' positions in the treatment planning CT images. An individual error is given to each coordinate of the tumor and the three markers as follows:

$$\boldsymbol{Y}_c'(P) = \boldsymbol{Y}_c(P) + \Delta \boldsymbol{Y}_{CT}(P), \tag{9}$$

$$\boldsymbol{X}_c'(P) = \boldsymbol{X}_c(P) + \Delta \boldsymbol{X}_{CT}(P). \tag{10}$$

After giving the variations, the regression coefficient $\boldsymbol{B}$ is obtained by means of PLSR when assuming the linear model $\boldsymbol{Y}_c' = \boldsymbol{X}_c' \boldsymbol{B}$.

Next, the intra-fractional variation $\Delta \boldsymbol{Y}_{intra}$ and $\Delta \boldsymbol{X}_{intra}$ are randomly given according to the normal distribution $N(0, \sigma_{intra}^2)$. In this study, σ_{intra} was set to 1.0 mm in order to simulate clinically possible variation

Table 1. The lung region of GTV location of each data, the time length of the log data, and the motion range of the four markers in the left–right (LR), superior–inferior (SI) and anterior–posterior (AP) directions. The difference of motion range of the marker indicated internal deformation in lung. LLL, left lower lobe; LUL, left upper lobe; RML, right middle lobe; RUL, right upper lobe

#	GTV location	length [sec]	Marker 1 LR/SI/AP [mm]	Marker 2 LR/SI/AP [mm]	Marker 3 LR/SI/AP [mm]	Marker 4 LR/SI/AP [mm]
1	RUL	197	3.6 / 8.6 / 8.1	3.5 / 6.9 / 6.9	3.0 / 10.6 / 8.7	2.9 / 7.7 / 6.2
2	LUL	100	2.6 / 3.7 / 3.3	5.0 / 2.0 / 2.9	3.8 / 3.6 / 3.3	5.4 / 2.1 / 3.8
3	LLL	138	1.8 / 3.1 / 6.1	3.8 / 8.1 / 5.8	3.9 / 9.0 / 6.1	4.0 / 10.1 / 7.2
4	LLL	165	3.3 / 8.5 / 3.1	3.5 / 10.2 / 1. 8	3.6 / 11.5 / 7.0	5.5 / 16.2 / 4.8
5	RML	275	1.5 / 13.1 / 4.2	2.5 / 11. 7 / 3.9	1.3 / 12.4 / 2.5	1.4 / 13.6 / 2.5
6	LLL	175	3.5 / 7.5 / 7.1	2.7 / 10.6 / 8.2	2.7 / 7.8 / 6.8	2.1 / 11.5 / 9.2
7	RUL	48	2.3 / 2.5 / 4.3	2.9 / 1.9 / 3.6	2.8 / 3.9 / 2.3	3.1 / 3.8 / 2.7
8	RUL	42	2.7 / 2.5 / 2.7	2.5 / 2.1 / 2.9	1.8 / 3.6 / 3.3	1.9 / 2.6 / 2.4
9	LLL	50	2.3 / 12.6 / 3.4	2.0 / 16.0 / 3.4	4.3 / 15.4 / 3.5	5.2 / 16.5 / 2.5
10	LLL	161	2.5 / 9.3 / 3.0	1.8 / 6.4 / 4.5	2.1 / 9.2 / 5.6	3.0 / 10.9 / 3.9

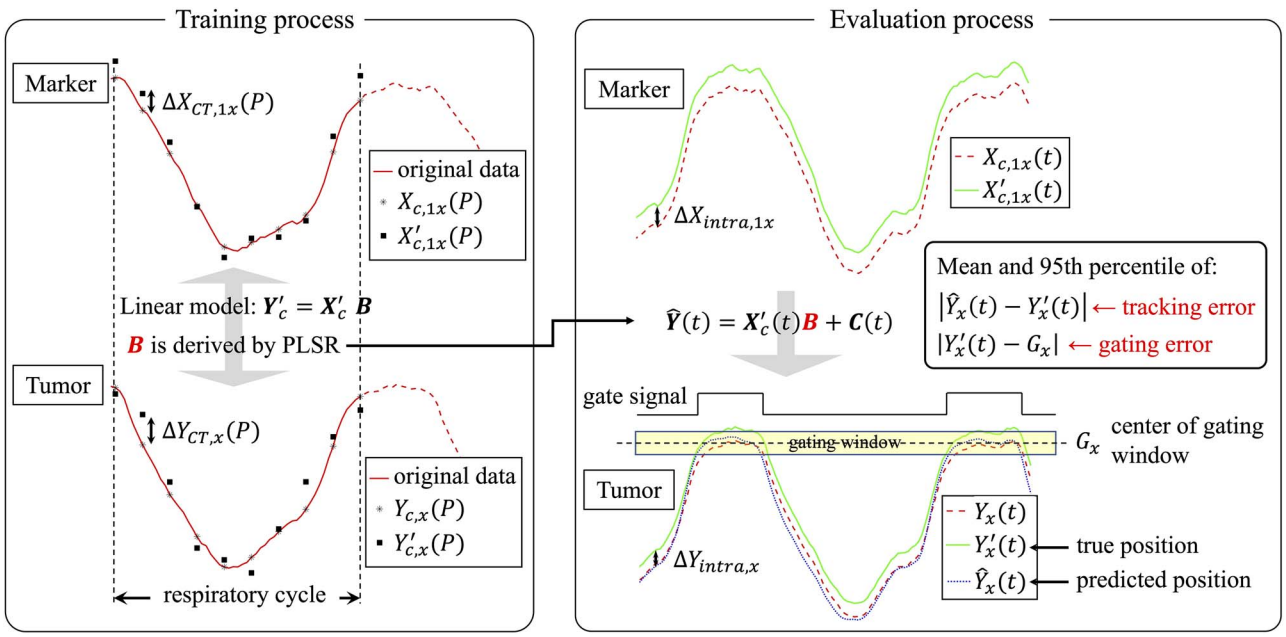

Fig. 2. Overview of the training process to derive the regression coefficients *B* and the evaluation process of the tracking error and the gating error. As for representative variables, component *x* of marker #1 and tumor are shown. Parameters with the subscripts *c* indicate that they are corrected with reference to *C*.

[17]. Each coordinate after variation is expressed as follows:

$$\boldsymbol{Y}'(t) = \boldsymbol{Y}(t) + \Delta\boldsymbol{Y}_{intra}, \tag{11}$$

$$\boldsymbol{X}'_c(t) = \boldsymbol{X}_c(t) + \Delta\boldsymbol{X}_{intra}. \tag{12}$$

$\boldsymbol{Y}'(t)$ is regarded as the ground truth of the tumor position. Finally, tumor position is predicted by $\hat{\boldsymbol{Y}}(t) = \boldsymbol{X}'_c(t)\boldsymbol{B} + \boldsymbol{C}(t)$.

In order to avoid evaluation with large variations that would be regarded as unacceptable variations in clinical practice, 2 × SD was set as the maximum value for any random error. The number of trials in random sampling was set to 100 since the fluctuation of the average and the SD of the evaluated error converged within 5% in more than 100 trials. Hence, 4000 trials that consisted of 10 patients' data—four situations for each datum by replacing the tumor assumed marker and 100 trials in random sampling—were conducted in total. The tracking error was evaluated in each trial by mean absolute error and 95th percentile of the absolute error between predicted position $\hat{\boldsymbol{Y}}(t)$ and the actual position $\boldsymbol{Y}'(t)$. The gating error was also evaluated by the same indices with assuming gated irradiation at the exhale respiratory phase. The gate signal is on only when the predicted tumor position $\hat{\boldsymbol{Y}}(t)$ is within the cubic region of ±2 mm, which is a typical setting for

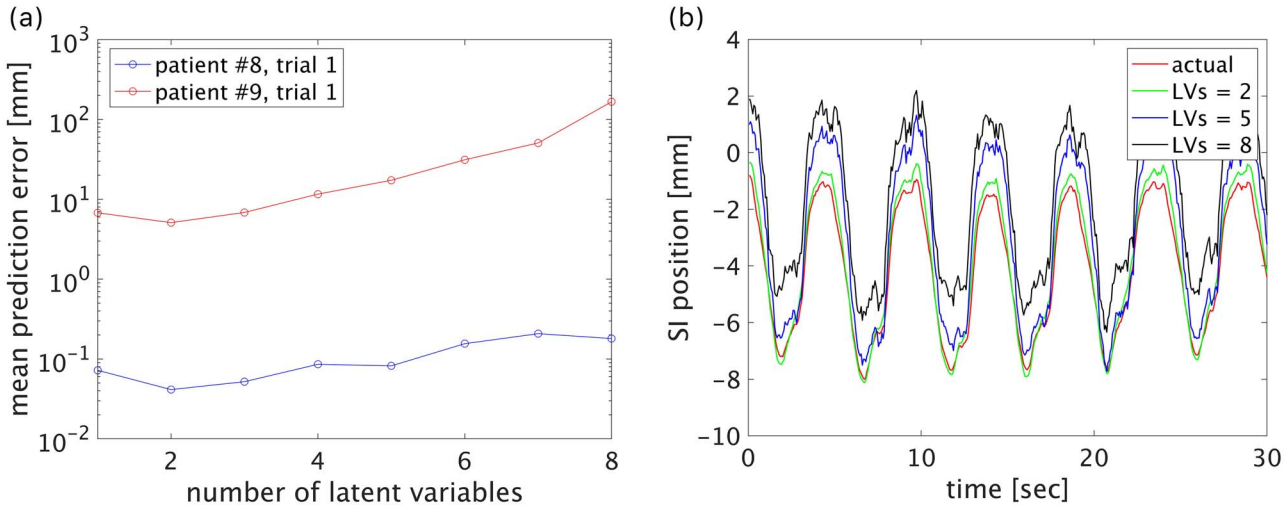

Fig. 3. (a) MPE in the training process. In patient #8 at trial #1 of random sampling, minimum tracking error of 0.4 mm in superior–inferior (SI) direction was obtained with number of LVs of 2. In patient #9 at trial #1, maximum tracking error of 4.9 mm in SI direction was obtained with number of LVs of 2. (b) An example of the actual position of the tumor assumed marker in SI direction predicted by PLSR with each LVs.

clinical practice, called gating window. The gating error was evaluated by the absolute displacement of the actual tumor position $\boldsymbol{Y}'(t)$ from the center of the gating window, defined as the position of the tumor-assumed marker at the exhale respiratory phase in the training data, during gate on.

For comparison, the tracking and gating errors were evaluated by rigid prediction and ordinally MLR prediction using three fiducial markers. In the rigid prediction, tumor position was determined by using fixed geometrical relationship of the tumor and the centroid position of three fiducial markers at the exhale respiratory phase in 4DCT. In the MLR prediction, regression coefficient matrix $\boldsymbol{B}$ was derived as $\boldsymbol{X}_c'^{-1}\boldsymbol{Y}_c'$ by solving pseudo-inverse matrix of $\boldsymbol{X}_c'$.

RESULTS

An example of MPE in the training process for each number of LVs is shown in Fig. 3a. In most cases, the minimum MPE was shown in the number of LVs from 1 to 3. Prediction of the tumor position by PLSR prediction with representative number of LVs in superior-inferior (SI) direction is shown in Fig. 3b. In this example, the optimum number of LVs was 2. When the number of LVs was large, the prediction tended to fluctuate due to overfitting and multicollinearity. From the above results, the maximum number of LVs of 3 was considered to be reasonable for this study. The ratio of the optimal number of LVs of 1, 2 and 3 were 26.5, 36.8 and 36.7%, respectively. It was thought that three principal LVs were sufficient to predict the tumor motion since most of explanatory variables and response variables are similar wave signals having same respiratory cycle.

Fig. 4 shows an example of actual and predicted tumor position by MLR, rigid and PLSR. The results for the data including large amplitude variation was shown in order to see the characteristics of each prediction method. In MLR prediction, predicted positions were

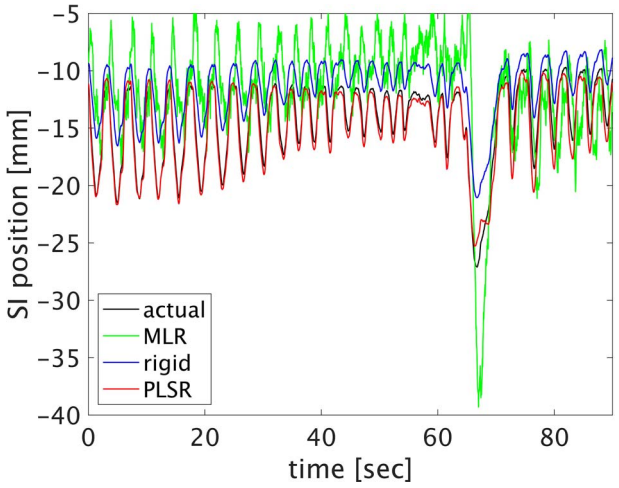

Fig. 4. An example of actual and predicted tumor position by MLR, rigid and PLSR.

fluctuated due to multicollinearity. In rigid prediction, since the geometrical relationship was fixed at the exhale respiratory phase, the variations were added as the offset. In the case of PLSR prediction, prediction accuracy was maintained even when the variations were given. In this example, a decrease of prediction accuracy due to σ_{CT} and σ_{intra} was suppressed in the PLSR prediction when compared with rigid prediction. In rigid prediction, the variations given to each explanatory variable are evenly contributed to the total prediction accuracy. On the other hand, the accuracy of the PLSR prediction is determined according to the variations to LVs. Hence, it is thought that the accuracy of PLSR predictions is not necessarily decreased the same as rigid prediction.

Table 2. Mean and 95th percentile of all trials in the tracking errors, which were evaluated by mean absolute error (MAE) and 95th percentile of absolute error (95AE), were summarized for each prediction method and each direction, left–right (LR), superior–inferior (SI) and anterior–posterior (AP)

	MAE [mm]						95AE [mm]					
	LR		SI		AP		LR		SI		AP	
	Mean	95th	Mean	95th	Mean	95th	Mean	95th	Mean	95th	Mean	95th
MLR	13.5	31.5	29.9	74.1	13.6	38.0	20.6	45.7	47.3	110.7	20.3	53.8
rigid	1.1	2.5	1.6	3.7	1.2	2.6	1.8	3.5	2.6	5.9	2.0	3.9
PLSR	1.0	2.2	1.2	2.6	1.0	2.4	1.5	2.8	1.9	3.7	1.6	3.1

Table 3. Mean and 95th percentile of all trials in the tracking errors, which were evaluated by mean absolute error (MAE) and 95th percentile of absolute error (95AE), were summarized for each patient in PLSR prediction

	MAE [mm]						95AE [mm]					
	LR		SI		AP		LR		SI		AP	
#	Mean	95th	Mean	95th	Mean	95th	Mean	95th	Mean	95th	Mean	95th
1	1.0	2.1	1.2	2.6	1.0	2.3	1.5	2.6	1.9	3.5	1.6	3.0
2	1.0	2.2	1.0	2.3	0.9	2.2	1.5	2.8	1.4	2.8	1.3	2.6
3	1.0	2.1	1.1	2.7	1.0	2.4	1.4	2.6	1.9	3.6	1.6	3.1
4	1.0	2.1	1.2	2.6	1.0	2.2	1.4	2.7	2.1	3.9	1.5	2.7
5	1.0	2.1	1.2	2.5	1.0	2.3	1.4	2.6	2.1	3.7	1.5	2.9
6	1.1	2.2	1.2	2.5	1.0	2.3	1.7	2.9	2.0	3.6	1.6	3.0
7	1.0	2.2	1.1	2.5	1.0	2.3	1.5	2.8	1.7	3.4	1.5	2.9
8	1.0	2.2	1.0	2.4	1.0	2.3	1.3	2.6	1.3	2.6	1.2	2.6
9	1.1	2.3	1.5	3.4	1.2	2.6	1.6	2.9	2.6	5.1	1.8	3.4
10	1.1	2.3	1.3	2.7	1.3	3.1	1.6	2.9	2.3	4.1	2.0	3.9
all	1.0	2.2	1.2	2.6	1.0	2.4	1.5	2.8	1.9	3.7	1.6	3.1

Mean and 95th percentile of the tracking errors are summarized in Table 2. The tracking errors of PLSR predictions were smaller than those of other prediction methods in all directions. The 95th percentile of all trials for MAE and 95th percentile of absolute error (95AE) were 2.6 mm and 3.7 mm, respectively, in PLSR prediction for SI direction. They were reduced by 1.1 mm and 2.2 mm by PLSR prediction compared with rigid prediction, respectively. The tracking errors in MLR were relatively large due to multicollinearity. The tracking errors by PLSR prediction for each patient are summarized in Table 3. The errors tended to be increased in the patient having large marker motion. It was though that the prediction accuracy in large motion which was not included in the training data set was decreased due to less linearity. As a result, the clinically applicable tracking accuracy could be achievable by PLSR for targeting the mobile tumors.

The gating errors are summarized in Table 4. The 95th percentiles of MAE and 95AE were 2.9 mm and 4.1 mm, respectively, in PLSR prediction for SI direction. Although improvement was moderate, 95th percentile values were reduced by PLSR prediction compared with rigid prediction.

The mean and SD of the gate efficiency, which was defined as the ratio of gate on time to total time, was 22.4 ± 20.2% in MLR prediction, 41.9 ± 20.7% in rigid prediction and 40.4 ± 19.6% in PLSR prediction. Since the estimated position fluctuated due to multicollinearity in MLR prediction, mean gate efficiency was less than those with other prediction methods. It was suggested that the clinically applicable accuracy could be achievable in respiratory-gated irradiation using PLSR prediction while maintaining the reasonable gate efficiency.

DISCUSSION

In this study, the tracking error and the gating error were evaluated assuming the possible variations of target/marker position determination in the CT images and the intra-fractional anatomical variation. One of the limitations in assessing the errors was that the variation was assumed to be only random errors without systematic errors. In an actual case, systematic errors, which may be specific on each treatment system, and others could be included. In general, the systematic error can be corrected since it can be regarded as a detectable offset. Hence the usefulness of the proposed technique is considered to be maintained when the systematic error is included. As for the variations, there are several other possibilities. One of the main variations that was not reproduced in this study was the error in marker coordinates calculation in the RTRT system. In actual treatment system, accuracy of the object tracking is expected to be about 0.2 mm when the marker tracking is performed correctly [19]. In this study, the reproduction of marker tracking error was ignored since the effect of marker tracking

Table 4. Mean and 95th percentile of all trials in the gating errors, which were evaluated by mean absolute error (MAE) and 95th percentile of absolute error (95AE), were summarized for each prediction method and each direction, left–right (LR), superior–inferior (SI) and anterior–posterior (AP)

	MAE [mm]						95AE [mm]					
	LR		SI		AP		LR		SI		AP	
	Mean	95th	Mean	95th	Mean	95th	Mean	95th	Mean	95th	Mean	95th
MLR	3.1	9.9	5.4	18.0	3.6	11.2	3.9	11.0	6.8	20.0	4.8	12.7
rigid	1.1	2.5	1.5	3.3	1.3	2.8	1.8	3.4	2.6	5.0	2.3	4.1
PLSR	1.1	2.5	1.4	2.9	1.3	2.7	1.8	3.4	2.5	4.1	2.3	3.9

error would be small compared with the other variations. Note that, each treatment system has the specific latency which causes delayed beam controlling and could have prediction function to compensate the latency. Actual irradiation accuracy should be assessed considering the system specifications.

In recent years, image processing techniques to detect tumor itself in kilovoltage [20, 21] or megavoltage [22, 23] images without the fiducial markers have been reported. It has also been reported that an anatomical feature such as the diaphragm could be used instead of the metal markers [24, 25]. These kinds of techniques are considered to be useful for patients who cannot have markers inserted. However, in cases when the image quality of the tumor is poor due to surrounding organs such as heart and/or vertebra, tumor detection may be difficult. Hence, it is necessary to use the fiducial markers or marker-less techniques depending on the situation.

As for clinical benefit of the PLSR prediction, the results suggested that the margin to compensate the variations and to make target volume could be reduced in tracking irradiation and gating irradiation. For instance, if both of σ_{CT} and σ_{intra} can be assured within 1 mm, the margin to compensate the variations of target delineation and intra-fractional anatomical variation would be about 3 or 4 mm in respiratory-gated irradiation. If necessary, by adding the additional margins to compensate the setup error, system specific latency and other possible error sources, target volume can be defined. In the current lung RTRT [2], the one marker closest to the tumor is tracked for beam gating. The gating error of the current RTRT can be assumed to be comparable to that of rigid prediction in this study. Hence, the target margin could be reduced by about 1 mm by using PLS prediction. Although the reduction may be moderate, PLSR prediction will be clinically effective since it is important to spare the organs at risk where possible, especially in hypofractionated radiation therapy.

Some confirmation processes will be required for the clinical use of the proposed technique. One is the confirmation of the marker size determined on the CT images in the treatment planning process. Unstable respiratory motion will introduce artifacts in CT images. In addition, metal artifacts may also induce uncertainty for the determination of the marker since it depends on the shape, size and mass of the marker [26]. The other is the confirmation of the geometrical relationship of the markers. Since the fiducial markers may drop after insertion [17], before the treatment, it should be confirmed that the change of geometrical relationships of the fiducial markers is within the tolerance. In addition, it is known that the range of respiratory motion during treatment could be varied from that during 4DCT acquisition [27]. Hence, if unacceptable discrepancy is found, it is recommended to create the regression model by acquiring the 4DCT again.

CONCLUSION

In this study, we proposed 3D tumor position prediction methods based on PLSR. The tracking and gating errors were evaluated, assuming the possible variations in clinical workflow by using the trajectory data of fiducial markers. The results suggested that the PLSR prediction can reduce the tracking/gating errors compared with rigid prediction. PLSR prediction with optimum number of LVs was robust to variations, and the clinically acceptable accuracy could be achievable for targeting mobile tumors. PLSR prediction is expected to be clinically applicable by confirming the geometrical change, such as inter-marker distance, before the treatment.

FUNDING

This work was partially supported by KAKENHI 18 K19887, 20H03612.

REFERENCES

1. Shirato, H, Shimizu, S, Kunieda, T et al. Physical aspects of a real-time tumor-tracking system for gated radiotherapy. *Int J Radiat Oncol Biol Phys.* 2000; 48(4):1187–95.
2. Inoue T, Katoh N, Onimaru R et al. Stereotactic body radiotherapy using gated radiotherapy with real-time tumor-tracking for stage I non-small cell lung cancer. *Radiat Oncol.* 2013;8:69–76.
3. Katoh, N, Onimaru, R, Sakuhara, Y et al. Real-time tumor-tracking radiotherapy for adrenal tumors. *Radiother Oncol.* 2008;87(3):418–24.
4. Suh, Y, Sawant, A, Venkat, R et al. Four-dimensional IMRT treatment planning using a DMLC motion-tracking algorithm. *Phys Med Biol.* 2009;54(12):3821–35.
5. Keall, PJ, Colvill, E, O'Brien, R et al. The first clinical implementation of electromagnetic transponder-guided MLC tracking. *Med Phys.* 2014;41(2):020702-1–020702-5.
6. Seppenwoolde, Y, Berbeco, RI, Nishioka, S et al. Accuracy of tumor motion compensation algorithm from a robotic respiratory tracking system: a simulation study. *Med Phys.* 2007;34(7):2774–84.

7. Hoogeman, M, Prevost, JB, Nuyttens, J et al. Clinical accuracy of the respiratory tumor tracking system of the cyberknife: assessment by analysis of log files. *Int J Radiat Oncol Biol Phys.* 2009;74(1):297–303.
8. Takayama, K, Mizowaki, T, Kokubo, M et al. Initial validations for pursuing irradiation using a gimbals tracking system. *Radiother Oncol.* 2009;93(1):45–9.
9. Depuydt, T, Verellen, D, Haas, O et al. Geometric accuracy of a novel gimbals based radiation therapy tumor tracking system. *Radiother Oncol.* 2011;98(3):365–72.
10. Berbeco, RI, Nishioka, S, Shirato, H et al. Residual motion of lung tumours in gated radiotherapy with external respiratory surrogates. *Phys Med Biol.* 2005;50(16):3655–67.
11. Ionascu, D, Jiang, SB, Nishioka, S et al. Internal-external correlation investigations of respiratory induced motion of lung tumors. *Med Phys.* 2007;34(10):3893–903.
12. Nakamura, M, Takamiya, M, Akimoto, M et al. Target localization errors from fiducial markers implanted around a lung tumor for dynamic tumor tracking. *Phys Med.* 2015;31(8):934–41.
13. Malinowski, KT, Pantarotto, JR, Senan, S et al. Inferring positions of tumor and nodes in Stage III lung cancer from multiple anatomical surrogates using four-dimensional computed tomography. *Int J Radiat Oncol Biol Phys.* 2010;77(5):1553–60.
14. Wold, S, Sjostrom, M, Eriksson, L. PLS-regression: a basic tool of chemometrics. *Chemometr Intell Lab.* 2001;58(2):109–30.
15. Takao, S, Miyamoto, N, Matsuura, T et al. Intrafractional Baseline Shift or Drift of Lung Tumor Motion During Gated Radiation Therapy With a Real-Time Tumor-Tracking System. *Int J Radiat Oncol Biol Phys.* 2016;94(1):172–80.
16. de Jong, S. SIMPLS: an alternative approach to partial least squares regression. *Chemometr Intell Lab.* 1993;18(3):251–63.
17. Imura, M, Yamazaki, K, Shirato, H et al. Insertion and fixation of fiducial markers for setup and tracking of lung tumors in radiotherapy. *Int J Radiat Oncol Biol Phys.* 2005;63(5):1442–7.
18. Tanabe, S, Umetsu, O, Sasage, T et al. Clinical commissioning of a new patient positioning system, SyncTraX FX4, for intracranial stereotactic radiotherapy. *J Appl Clin Med Phys.* 2018;19(6):149–58.
19. Miyamoto, N, Ishikawa, M, Sutherland, K et al. A motion-compensated image filter for low-dose fluoroscopy in a real-time tumor-tracking radiotherapy system. *J Radiat Res.* 2015;56(1):186–96.
20. Hirai R, Sakata Y, Tanizawa A et al. Real-time tumor tracking using fluoroscopic imaging with deep neural network analysis. *Phys Med.* 2019;59:22–9.
21. Bhusal Chhatkuli, R, Demachi, K, Uesaka, M et al. Development of a markerless tumor-tracking algorithm using prior four-dimensional cone-beam computed tomography. *J Radiat Res.* 2019;60(1):109–15.
22. Rottmann, J, Keall, P, Berbeco, R. Markerless EPID image guided dynamic multi-leaf collimator tracking for lung tumors. *Phys Med Biol.* 2013;58(12):4195–204.
23. Zhang, X, Homma, N, Ichiji, K et al. Tracking tumor boundary in MV-EPID images without implanted markers: a feasibility study. *Med Phys.* 2015;42(5):2510–23.
24. Cervino, LI, Chao, AK, Sandhu, A et al. The diaphragm as an anatomic surrogate for lung tumor motion. *Phys Med Biol.* 2009;54(11):3529–41.
25. Zhou, D, Quan, H, Yan, D et al. A feasibility study of intrafractional tumor motion estimation based on 4D-CBCT using diaphragm as surrogate. *J Appl Clin Med Phys.* 2018;19(5):525–31.
26. Miyamoto N, Maeda K, Abo D et al. Quantitative evaluation of image recognition performance of fiducial markers in real-time tumor-tracking radiation therapy. *Phys Med.* 2019;65:33–9.
27. Harada, K, Katoh, N, Suzuki, R et al. Evaluation of the motion of lung tumors during stereotactic body radiation therapy (SBRT) with four-dimensional computed tomography (4DCT) using real-time tumor-tracking radiotherapy system (RTRT). *Phys Med.* 2016;32(2):305–11.